

Use of dual-tree complex wavelet packet transform to generate tri-component thunderstorm wind records

Y.X. Liu ¹, H.P. Hong ²

¹*Department of Civil and Environmental Engineering, University of Western Ontario, London, Ontario N6A 5B9, Canada, Email: yliu3863@uwo.ca*

²*Department of Civil and Environmental Engineering, University of Western Ontario, London, Ontario N6A 5B9, Canada, Email: hongh@eng.uwo.ca*

SUMMARY:

Strong thunderstorm winds cause damage to structures. However, the available number of tri-component thunderstorm wind records with a subsecond sampling interval for structural dynamic analysis is limited. In the present study, the use of the dual-tree complex wavelet packet transform (DT- \mathcal{C} WPT) to generate tri-component nonstationary non-Gaussian thunderstorm wind records is proposed. The use of DT- \mathcal{C} WPT is to gain efficiency since it is a redundant transform with a low redundancy factor and provides phase information. The generation is seed-record- or data-driven and is based on the overall framework of the iterative power and amplitude correction algorithm. This ensures that the sampled records match the prescribed marginal (mixture) cumulative distribution of each record component as well as the crossed and non-crossed time-frequency-dependent power spectra density functions. The use of the proposed approach is shown by numerical examples, illustrating its efficiency and the statistics of the sampled nonstationary non-Gaussian processes agreeing well with their targets.

Keywords: Record-based simulation, tri-component thunderstorm wind, dual-tree complex wavelet packet transform

1. INTRODUCTION

The time-frequency contents of the wind can be important for analyzing wind-sensitive structures. It is known that low-frequency wind (i.e., temporal-averaged wind speed with a duration of about 30 s) and its corresponding direction in the alongwind orientation from a thunderstorm event varies in time. The fluctuating winds (i.e., high-frequency component winds) in three orthogonal orientations are also time-varying. However, the wind records in three orthogonal directions with a high sampling rate, at a point in space, are available only for a few locations and a small number of thunderstorm events (e.g., Lombardo et al. 2014; Solari et al. 2015; Burlando et al. 2018; Huang et al. 2019). The analysis of such wind is often carried out by separating the wind record into time-varying mean and fluctuating wind components, which is often modelled as a uniformly modulated evolutionary process (e.g., Chen and Letchford 2007; Tubino and Solari 2020). The use of the S-transform (ST) and (discretized) continuous wavelet transform to analyze the time-frequency contents of the thunderstorm wind was considered in several studies (e.g., Hong et al. 2021a, b, 2022; Brusco et al. 2022). Zhang et al. (2019) reported the statistics of the thunderstorm wind speed in the alongwind orientation. A complete model that can be used to simulate the tri-component thunderstorm winds in three orthogonal directions is unavailable.

To overcome the lack of sufficient records to develop the model for simulating thunderstorm wind records, the seed-record- or data-driven approach to sample wind speed in a direction has been considered in the literature (e.g., Wang et al. 2013; Kwon and Kareem 2019; Wang and Wu 2021). Some of the available studies used the discrete wavelet transform (DWT) and discrete wavelet packet transform (DWPT); none of them dealt with the simulation of the tri-component winds. The drawbacks of DWT and DWPT are oscillations, shift variance, aliasing, and lack of directionality (Selesnick et al. 2005; Bayram and Selesnick 2008), which could be overcome by using the dual-tree complex DWT (DT- \mathcal{C} WT), and the dual-tree complex DWPT (DT- \mathcal{C} WPT) (Bayram and Selesnick 2008). By applying the iterative power and amplitude correction (IPAC) algorithm (Hong et al. 2021a, b, 2022) with modification, Liu and Hong (2022) used ST and continuous wavelet transform (CWT) to simulate multi-component thunderstorm winds with nonstationary non-Gaussian characteristics and the crossed and non-crossed time-frequency dependent power spectral density (TFPSD) functions. However, the use of ST and CWT in such a setting can be computing time-consuming if the simulation of a long-duration wind speed record is required.

In the present study, the use of DT- \mathcal{C} WPT to generate tri-component nonstationary non-Gaussian thunderstorm wind records is proposed. The use of DT- \mathcal{C} WPT is to gain efficiency since it is a redundant transform with a low redundancy factor and provides phase information. The generation is seed-record- or data-driven and is based on the overall framework of the IPAC algorithm. The use of this algorithm ensures that the sampled multi-component records match the prescribed marginal (mixture) cumulative distribution function (CDF) of each record component as well as the crossed and non-crossed TFPSD functions. In the following, the use of DT- \mathcal{C} WPT within the IPAC algorithm framework is explained, and illustrated by numerical examples.

2. USE OF DUAL-TREE COMPLEX DISCRETE WAVELET PACKET TRANSFORM

DT- \mathcal{C} WT is approximately shift-invariant and has a redundancy factor of 2 for a one-dimensional signal. The use of the two-band DWT in DT- \mathcal{C} WT to decompose a signal might not be “optimal” – a problem that could be overcome by DT- \mathcal{C} WPT (Bayram and Selesnick 2008). Similar to DT- \mathcal{C} WT, DT- \mathcal{C} WPT also uses the lower and upper trees for the real and imaginary parts of the transform. DT- \mathcal{C} WPT coefficient for a real signal $x_p(t)$, $x_{DT-\mathcal{C}WPT,p}(j,k)$, is expressed as,

$$x_{DT-\mathcal{C}WPT,p}(j,k) = x_{h,DT-\mathcal{C}WPT,p}(j,k) + ix_{g,DT-\mathcal{C}WPT,p}(j,k) \quad (1)$$

where $x_{h,DT-\mathcal{C}WPT,p}(j,k)$ and $x_{g,DT-\mathcal{C}WPT,p}(j,k)$ are the coefficients from the upper and lower trees. The amplitude and phase of $x_{DT-\mathcal{C}WPT,p}(j,k)$ are represented as $|x_{DT-\mathcal{C}WPT,p}(j,k)|$ and $\phi_{DT-\mathcal{C}WPT,p}(j,k) = \arg(x_{DT-\mathcal{C}WPT,p}(j,k))$, respectively. For simplicity, DT- \mathcal{C} WPT and its inverse are denoted as $x_{DT-\mathcal{C}WPT,p} = F_{DT-\mathcal{C}WPT}(x_p(t))$, and $x_p(t) = F_{DT-\mathcal{C}WPT}^{-1}(x_{DT-\mathcal{C}WPT,p})$. The TFPSD function based on DT- \mathcal{C} WPT can be defined as, $S_{DT-\mathcal{C}WPT,pp}(j,k) = x_{DT-\mathcal{C}WPT,p}(j,k)x_{DT-\mathcal{C}WPT,p}^*(j,k)/2$; its use is energy preserving ($\sum_{j,k} x_{DT-\mathcal{C}WPT,p}(j,k)x_{DT-\mathcal{C}WPT,p}^*(j,k)/2 = \sum_k |x(t_k)|^2$). To present $S_{DT-\mathcal{C}WPT,pp}(j,k)$,

the sequential order arrangement (Wickerhauser 1994) will be considered. Given two processes $x_p(t)$ and $x_q(t)$, the coherence function $\Gamma_{DT-\mathcal{C}WPT,pq}(j,k)$ based on DT- \mathcal{C} WPT coefficients is,

$$\Gamma_{DT-\mathcal{C}WPT,pq}(j,k) = S_{DT-\mathcal{C}WPT,pq}(j,k) / \sqrt{S_{DT-\mathcal{C}WPT,pp}(j,k)S_{DT-\mathcal{C}WPT,qq}(j,k)}, \quad (2)$$

where $S_{DT-\mathcal{C}WPT,pq}(j,k) = x_{DT-\mathcal{C}WPT,p}(j,k)x_{DT-\mathcal{C}WPT,q}^*(j,k)/2$. $|\Gamma_{DT-\mathcal{C}WPT,pq}(j,k)|$ is known as lagged coherence, and its corresponding phase spectra is $\Phi_{DT-\mathcal{C}WPT,pq}(j,k) = \arg(\Gamma_{DT-\mathcal{C}WPT,pq}(j,k))$. As an

illustration, the evaluated TFPSD and coherence functions by using DT- \mathcal{C} WPT for the tri-component thunderstorm winds shown in Figures 1a to 1c are illustrated in Figures 1d to 1l. The marginal CDFs of the record are also shown in Figure 1, indicating non-Gaussian characteristics.

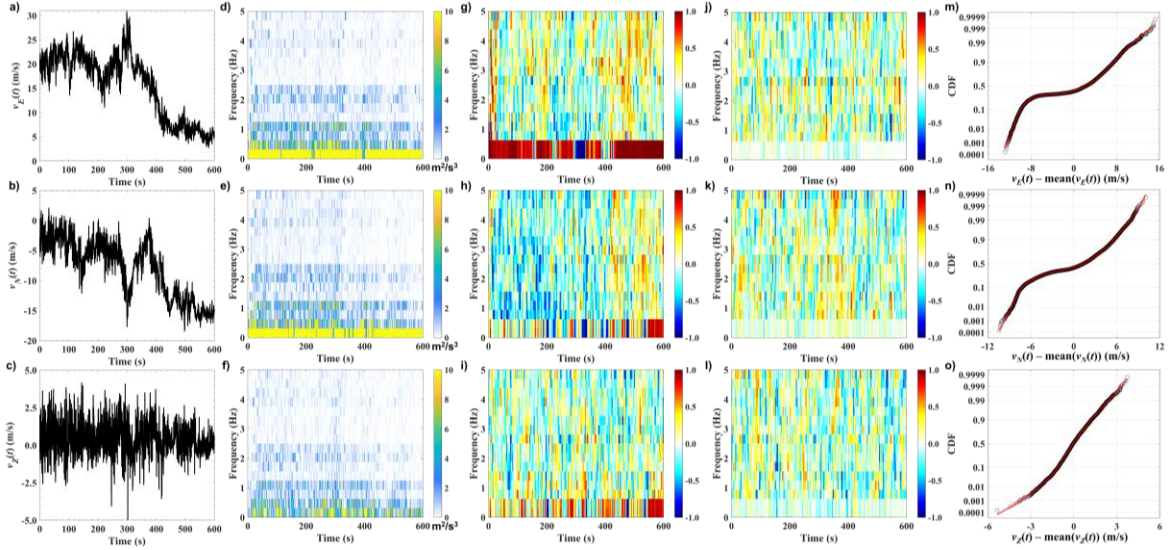


Figure 1. *a-c*) thunderstorm wind recorded on 2011.12.16 (anemometer 1, the Port of Livorno (Bulando et al. 2018)) for $v_E(t)$, $v_N(t)$, and $v_Z(t)$ (west, south, and upward winds are positive); *d-f*) TFPSD for $v_E(t)$, $v_N(t)$, and $v_Z(t)$; *g-i*) (*j-l*) the real (imaginary) part of the coherence between $v_E(t)$ and $v_N(t)$, $v_E(t)$ and $v_Z(t)$, and $v_N(t)$ and $v_Z(t)$; *m-o*) fitted marginal mixture CDF for $v_E(t)$, $v_N(t)$, and $v_Z(t)$.

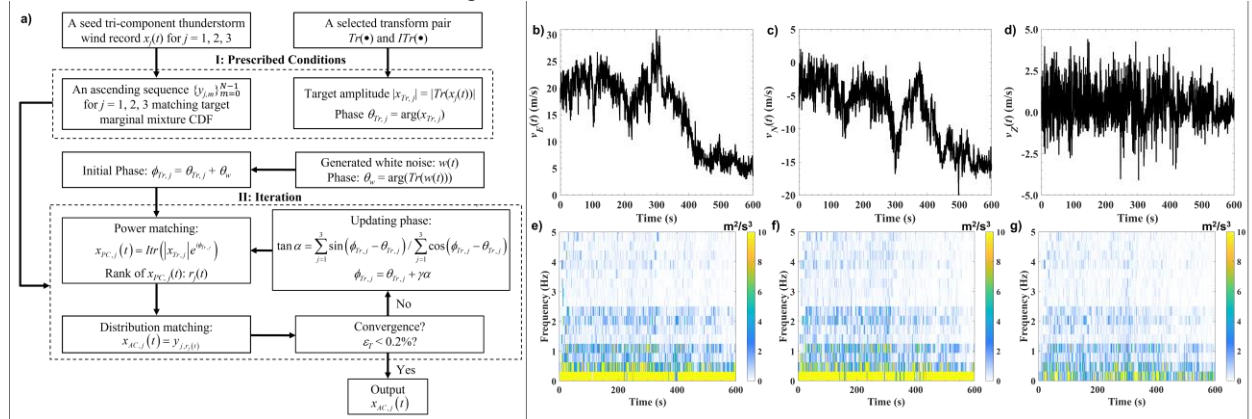


Figure 2. *a*) the schematic of the IPAC algorithm; *b-d*) typical sampled $v_E(t)$, $v_N(t)$ and $v_Z(t)$, respectively; *e-g*) mean of the TFPSD functions of sampled $v_E(t)$, $v_N(t)$, and $v_Z(t)$, respectively (based on 5000 sets of samples).

3. GENERATION OF TRI-COMPONENT WIND RECORD

The overall framework of the IPAC algorithm (Hong et al. 2021b; Cui and Hong 2021) with a slight modification (Liu and Hong 2022) is used for the simulation of the nonstationary non-Gaussian thunderstorm winds by adopting DT- \mathcal{C} WPT. The modification is aimed at improving the matching of the coherence (i.e., the phase difference) between each pair of the processes of the seed tri-component thunderstorm record; the schematic of the algorithm is illustrated in Figure 2a. To illustrate the use of the IPAC algorithm with DT- \mathcal{C} WPT, we use the tri-component records shown in Figures 1a to 1c as the seed records to sample 5000 sets of tri-component records. A typical set is shown in Figures 2b to 2d. The mean of the estimated TFPSD function is shown in Figures 2e to 2g for $v_E(t)$, $v_N(t)$, and $v_Z(t)$, indicating that they agree well with their targets. Note that the matching of the marginal CDFs is ensured by the algorithm. An inspection of the results

indicates that the matching of the coherence is also adequate (the results are not shown due to space limitation). Moreover, our experience shows that the ratio of the computing time for simulating tri-component winds similar to those shown in Figures 2b to 2d is 2.6:60:1 by using CWT with the harmonic wavelet, ST, and DT- \mathcal{C} WPT.

4. CONCLUSIONS

We proposed the use of the dual-tree complex wavelet packet transform (DT- \mathcal{C} WPT) to generate tri-component nonstationary non-Gaussian thunderstorm wind records. The use of DT- \mathcal{C} WPT is to gain efficiency since it is a redundant transform with a low redundancy factor and provides phase information. The generation is data-driven and is based on the overall framework of the IPAC algorithm. Numerical examples are provided, indicating the proposed approach can generate tri-component thunderstorm winds that match the prescribed marginal CDFs of the components, the crossed and non-crossed TFPSD functions. The use of the proposed approach is very efficient.

REFERENCES

- Bayram, I., & Selesnick, I. W. (2008). Overcomplete discrete wavelet transforms with rational dilation factors. *IEEE Transactions on Signal Processing*, 57(1), 131-145.
- Brusco, S., Buresti, G., & Piccardo, G. (2022). Thunderstorm-induced mean wind velocities and accelerations through the continuous wavelet transform. *Journal of Wind Engineering and Industrial Aerodynamics*, 221, 104886.
- Burlando, M., Zhang, S., & Solari, G. (2018). Monitoring, cataloguing, and weather scenarios of thunderstorm outflows in the northern Mediterranean. *Natural Hazards and Earth System Sciences*, 18(9), 2309-2330.
- Chen, L., & Letchford, C. W. (2007). Numerical simulation of extreme winds from thunderstorm downbursts. *Journal of Wind Engineering and Industrial Aerodynamics*, 95(9-11), 977-990.
- Cui, X.Z., & Hong, H.P. (2021). Simulating nonstationary and non-Gaussian vector ground motions with time-and frequency-dependent lagged coherence. *Earthquake Engineering & Structural Dynamics*, 50(9), 2421-2441.
- Hong, H.P., Cui, X.Z., & Qiao, D. (2021a). An algorithm to simulate nonstationary and non-Gaussian stochastic processes. *Journal of Infrastructure Preservation and Resilience*, 2(1), 1-15.
- Hong, H.P., Cui, X.Z., & Xiao, M.Y. (2021b). Modelling and simulating thunderstorm/downburst winds using S-transform and discrete orthonormal S-transform. *J. of Wind Eng. and Industrial Aerodynamics*, 212, 104598.
- Hong, H.P., Cui, X.Z., & Qiao, D. (2022). Simulating nonstationary non-Gaussian vector process based on continuous wavelet transform. *Mechanical Systems and Signal Processing*, 165, 108340.
- Huang, G., Jiang, Y., Peng, L., Solari, G., Liao, H., & Li, M. (2019). Characteristics of intense winds in mountain area based on field measurement: Focusing on thunderstorm winds. *J. of W. Eng. & Ind. Aerody.*, 190, 166-182.
- Kwon, D.K., & Kareem, A. (2019). Towards codification of thunderstorm/downburst using gust front factor: Model-based and data-driven perspectives. *Engineering Structures*, 199, 109608.
- Liu, Y.X., & Hong, H.P. (2022). Data-driven approach for generating tri-component nonstationary non-Gaussian thunderstorm wind records using continuous wavelet transforms and S-transform. Under review for publication.
- Lombardo, F.T., Smith, D. A., Schroeder, J.L., & Mehta, K.C. (2014). Thunderstorm characteristics of importance to wind engineering. *Journal of Wind Engineering and Industrial Aerodynamics*, 125, 121-132.
- Selesnick, I.W., Baraniuk, R.G., & Kingsbury, N.C. (2005). The dual-tree complex wavelet transform. *IEEE signal processing magazine*, 22(6), 123-151.
- Solari, G., De Gaetano, P., & Repetto, M.P. (2015). Thunderstorm response spectrum: fundamentals and case study. *Journal of Wind Engineering and Industrial Aerodynamics*, 143, 62-77.
- Tubino, F., & Solari, G. (2020). Time varying mean extraction for stationary and nonstationary winds. *Journal of Wind Engineering and Industrial Aerodynamics*, 203, 104187.
- Wang, H., & Wu, T. (2021). Fast Hilbert-wavelet simulation of nonstationary wind field using noniterative simultaneous matrix diagonalization. *Journal of Engineering Mechanics*, 147(3), 04020153.
- Wang, L., McCullough, M., & Kareem, A. (2013). A data-driven approach for simulation of full-scale downburst wind speeds. *Journal of Wind Engineering and Industrial Aerodynamics*, 123, 171-190.
- Wickerhauser, M. V. (1994). Large-rank approximate principal component analysis with wavelets for signal feature discrimination and the inversion of complicated maps. *J. of Chemical Inf. and Comp. Sc.*, 34(5), 1036-1046.
- Zhang, S., Solari, G., Burlando, M., & Yang, Q. (2019). Directional decomposition and properties of thunderstorm outflows. *Journal of Wind Engineering and Industrial Aerodynamics*, 189, 71-90.